Influence of the four-spin exchange interaction on the magnetic properties of manganites

INSTITUTE OF PHYSICS PUBLISHING JOURNAL OF PHYSICS: CONDENSED MATTER

J. Phys.: Condens. Matter **17** (2005) 5881–5888 doi:10.1088/0953-8984/17/37/023

Influence of the four-spin exchange interaction on the magnetic properties of manganites

S S Aplesnin[1,2] **and N I Piskunova**[1]

[1] M F Reshetneva Aircosmic Siberian State University, Krasnoyarsk 660036, Russia
[2] L V Kirensky Institute of Physics, Siberian Branch of the Russian Academy of Science, Krasnoyarsk 660036, Russia

Received 20 June 2005, in final form 11 August 2005
Published 2 September 2005
Online at stacks.iop.org/JPhysCM/17/5881

Abstract

It is shown that non-Heisenberg exchange interaction should be taken into account to reproduce the magnetic phase diagram of $La_{1-x}A_xMnO_3$ (A = Ca, Sr) using only effective exchange parameters and spins. The formation of the four-spin exchange arises from carrier hopping and coincides with the critical concentration metal–dielectric transition. The two- and four-spin exchange parameters are determined by Monte Carlo simulations.

(Some figures in this article are in colour only in the electronic version)

1. Introduction

The manganites $Re_{1-x}A_xMnO_3$ (where Re = La, Pr, Nd, etc and A = Ca, Sr, Ba, etc) have been at the centre of attention in condensed matter for the last two decades because of the variety and novelty of electronic phenomena in them and the possibility of applications in spintronics. The initial interest was sparked by the discovery of colossal magnetoresistance. Subsequent work has been shown a variety of magnetic phases, phase transitions and phenomena depending on the doping x, temperature, and ionic species Re and A as well as external perturbations. The change of the kind of magnetic ordering from antiferromagnetic to ferromagnetic is observed at $x = 0.08$–0.09 in $La_{1-x}A_xMnO_3$ (A = Ca, Sr) [1]. The ferromagnetic dielectric becomes a ferromagnetic metal with colossal magnetoresistance near T_c for $x > 0.2$. The early simulations explored the competition between (double exchange induced) ferromagnetism and antiferromagnetic (super) exchange.

However, Millis [2] has shown that the 'double exchange' model disagreed with several experimental results by an order of magnitude or more. The discrepancy was resolved by including polaron effects due to a very strong electron–phonon coupling coming from a Jahn–Teller splitting of the Mn^{3+} ion. The measurements of specific heat also indicate an anomalous softening of the lattice arising from the T^3-term in the specific heat in a fairly wide x region ($0.1 < x < 0.3$) [3], but this is not apparently relevant to the crystal (rhombohedral–orthorhombic) transition. This anomaly is ascribed to the subsisting dynamic Jahn–Teller

distortion down to low or zero temperature. The strong coupling with the lattice may induce major four-spin exchange interaction (A), the value of which is $AS^4 \sim \frac{1}{Ma^2}(\frac{\nabla J}{\theta_D})^2$, where θ_D is the Debye temperature ($\theta_D = 320$–450 K) [4], $M \sim 10^{-22}$ g, $a \sim 4 \times 10^{-10}$ m, S is changed from $S = 2$ to 3/2 with doping. The four-spin exchange interaction resulting from the exchange by virtual phonons is $A \sim 0.1$ meV for $(\nabla J/\theta_D) \sim 0.03$. The relevant contribution to the four-spin exchange interaction can be given by the interaction (I_{s-d}) of a moving electron with a localized one. Using the small parameter W/E_g (W is the bandwidth, E_g is the gap), the Heisenberg exchange (J), four spin exchange interaction (A) and ratio (J/A) were estimated to be $J \sim I_{s-d}^2 W^2/E_g^3$, $A \sim I_{s-d}^4 W^4/E_g^7$, $J/A \sim I_{s-d}^2 W^2/E_g^4$ respectively. With doping, the gap in the single-electron excitation spectrum decreases and the non-Heisenberg exchange value may be compared with the value of bilinear exchange. So the $e_g(\sigma^*)$ band is about 1 eV wide, and the t_{2g}–e_g separation is about 1.5 eV [5]; I_{s-d} is (0.5–1) eV.

Another problem in manganites is that the isotherms H/M never intercept the M^2 axis, even at temperatures much lower than the temperature of the minimum in $\partial M/\partial T$. The extrapolation from low field, where the approximation is justified, does not cut the M^2 axis either. This makes it impossible to define the order parameter. Moreover, the isotherms never reach the origin; they intercept the H/M axis at a finite value, giving a fixed susceptibility [6]. Because of this, the magnetic transition outside the range $0.275 < x < 0.43$ is not a true phase transition [6], and is unlike the common continuous magnetic phase transition.

2. Model and results discussion

The magnetic properties are simulated in the Heisenberg model with random exchange interactions.

$$H = -\sum_{i,j}^{L} J_{i,j} S_i S_j - \sum_{i,j}^{L} A_{i,j,k,l}(S_i S_j)(S_k S_l) \tag{1}$$

where J_{ij} is the exchange between nearest neighbours, $A_{i,j,k,l}$ is the four-spin exchange interaction, spin $\mathbf{S}_i$ is treated as a continuous vector $\mathbf{S}$ ($S\cos\theta$, $S\sin\theta\sin\varphi$, $S\sin\theta\cos\varphi$) with the polar angles $\{\theta, \varphi\}$ characterizing the orientation of the spin $\mathbf{S}_i$, and L is size of the cube. Quantum effects can be neglected since $S > 1$. Manganites have the perovskite-type crystal structure, in which the rare-earth ions locate in the centre of the cube and manganese ions are at the cube vertices. If at the left and at the right of the cube face the various valence ions are found, then exchange interactions between the nearest manganese ions are equal to $J = K$ ($K > 0$) and four-spin exchange ($A > 0$) arises, as shown in figure 1 by the bold solid line. La^{3+} and $Ca^{2+}(Sr)^{2+}$ ions are plotted by solid and empty circles. The magnetic structure of $LaMnO_3$ consists of the ferromagnetic ordering spins in the plane ($J_{xy} > 0$) which ordered antiferromagnetically ($J_z < 0$). The ratio of the exchange parameters has been determined from the spin dynamics as a result of a fit of the dispersion of spin waves using a Heisenberg model with the four first in-plane neighbour couplings (J_1) (ferromagnetic) to J_{AF}—antiferromagnetic along [001]—$J_{AF}/J_1 \approx -0.7$ and an effective single-ion anisotropy $D/J_1 = 0.2$ for $LaMnO_3$ [7].

A Monte Carlo (MC) procedure was performed on the cubic lattice with $18 \times 18 \times 18$ sites and periodical boundary conditions. We used 16 000–28 000 MC/spin. Substitution of ions was realized in the lattice by using random numbers. The root-mean-square error does not exceed the symbol size plotted in the figures. Averaging over ten configurations of impurities distribution gives an error within the limit of a few per cent near the critical concentration.

To clarify the relationship between the metal–insulator transition and the percolation of carriers inducing the ferromagnetic exchange on the cube surface separating La^{3+} and

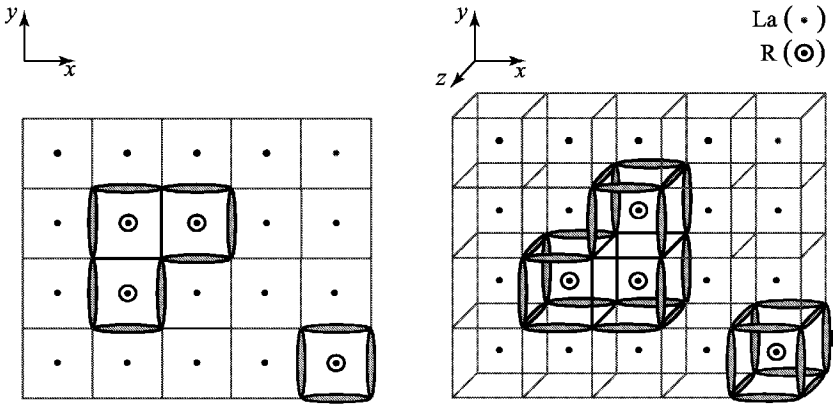

Figure 1. Random distribution of the rare-earth ions (Ca, Sr) in the lattice and induced ferromagnetic exchange (K), four-spin exchange (A) noted by double line.

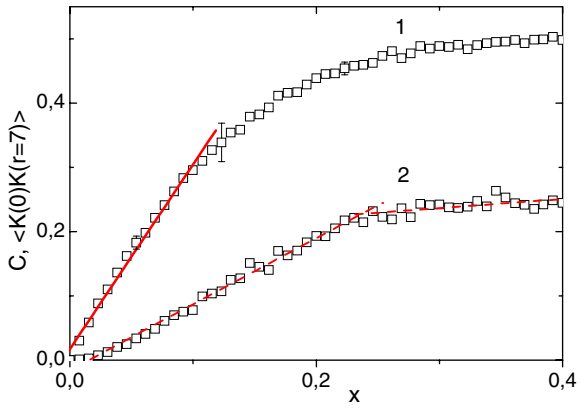

Figure 2. Concentration of K-bonds (1) and their correlator $\langle \mathrm{K}(0)\mathrm{K}(r = 7)\rangle$ (2) at the distance $r/a = 7$ along [001] versus bivalent A = Sr, Ca ion concentration.

R^{2+} ions we calculated the K-bond concentration and $\langle \mathrm{K}(0)\mathrm{K}(r)\rangle$ correlation function at the distance $r = 7a$; these are presented in figure 2. According to our model the concentration (c) of K-bonds exceeds the impurity concentration (x), as shown in figure 2. The calculated data are interpolated by the linear function $c = 2.9x$ for $x < 0.1$. Concentration of K-bonds and their correlation value $\langle K(0)K(r)\rangle$ approach the saturation state at $x > x_{c2} H 0.24$ that is illustrated in figure 2 by a dotted line. The value $x_{c2} = 0.24(2)$ found is in agreement with experimental data $x_{c2}^{ex} = 0.225$ [4] at which the metal–insulator transition is observed in $La_{1-x}Ca_xMnO_3$. Our model confirms the picture of nanoscale phase separation of electron density in manganites [3] and the coexistence of the two kinds of magnetic domains with ferromagnetic K-bonds and antiferromagnetic J-bonds that become frustrated at large concentrations of R^{2+} ions. Replacement of the interlayer J_{AF}-bond by ferromagnetic exchange causes the disappearance of AF long-range order at the critical concentration (x_{c1}) that is determined by the derivative of the magnetization and the change in the sign of the spin–spin correlation function from negative to positive along [001] direction. The magnetization and spin–spin correlation functions are shown in figure 3. The phase diagram of the ground state of antiferromagnetic and ferromagnetic long-range order is given in figure 4. On increasing the K-bond value the AF region decreases and the critical concentration tends to a constant value $x_{c1} = 0.04 \pm 0.015$ at $K/J > 4$. The critical concentrations and ferromagnetic exchanges

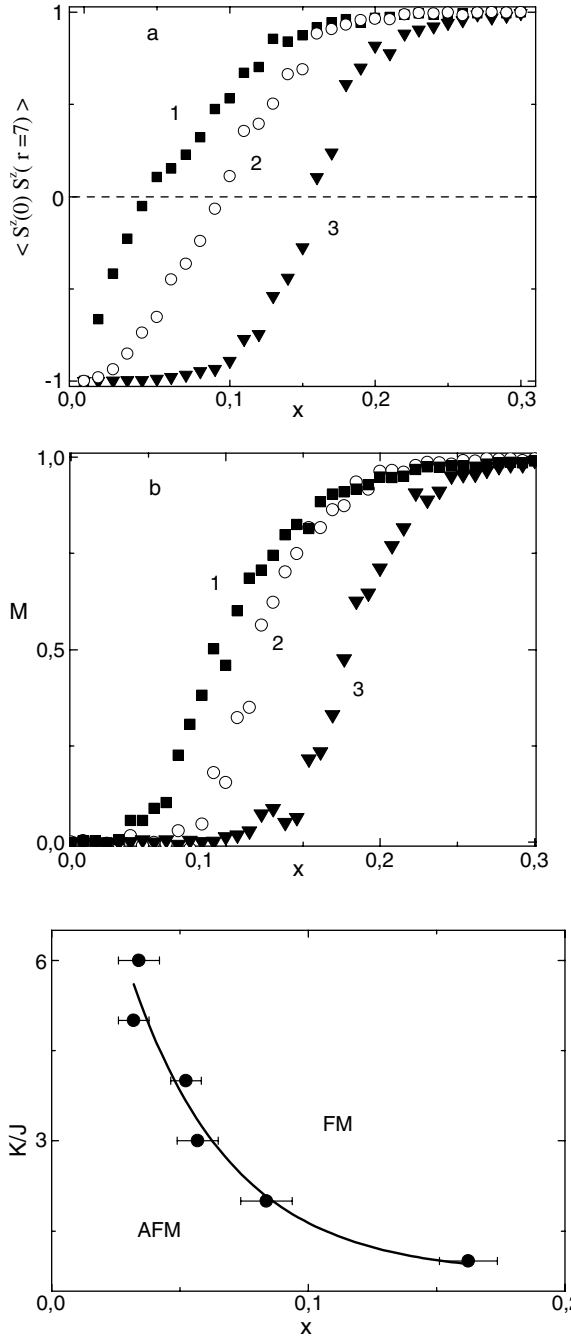

Figure 3. Spin–spin correlation function $\langle S^z(0)S^z(r = 7)\rangle$ simulated at $r/a = 7$ along [001] (a) and magnetization M (b) versus bivalent A = Sr, Ca ion concentration at $K/J = 6$ (1), 2(2), 1(3).

Figure 4. Phase diagram of the ground state of antiferromagnetic (AFM) and ferromagnetic (FM) in-plane K/J-bivalent A = Sr, Ca ion concentration.

values corresponding to the phase transition from AFM to FM are equal to $x_{c1} = 0.08 \pm 0.01$, $K \approx 2J$ for $La_{1-x}Ca_xMnO_3$ and $x_{c1} = 0.06 \pm 0.01$, $K \approx 3J$ for $La_{1-x}Sr_xMnO_3$.

The Néel and Curie temperatures were calculated from the temperature dependences of the spin–spin correlation function and magnetization presented in figure 5. The Curie temperatures of the ferromagnet at various values of the four-spin exchange are given in figure 6. The $T_c(A)$

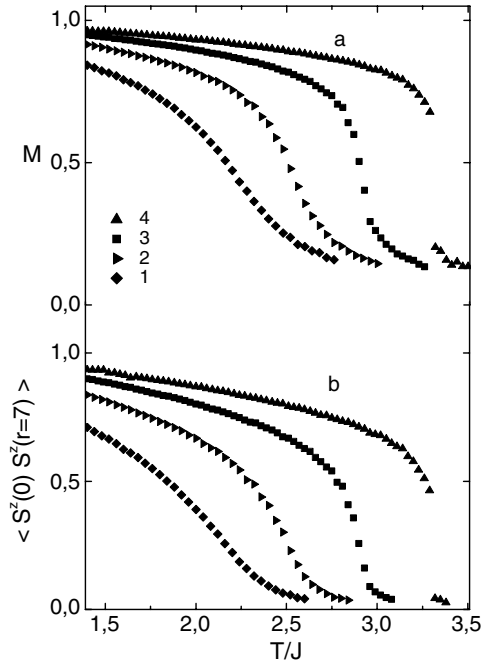

Figure 5. Magnetization (M) (a), and spin–spin correlation function $\langle S^z(0)S^z(r = 7)\rangle$ (b) versus temperature for $x = 0.3$, $A/K = 0.15$ (1), 0.3 (2), 0.45 (3), 0.6 (4).

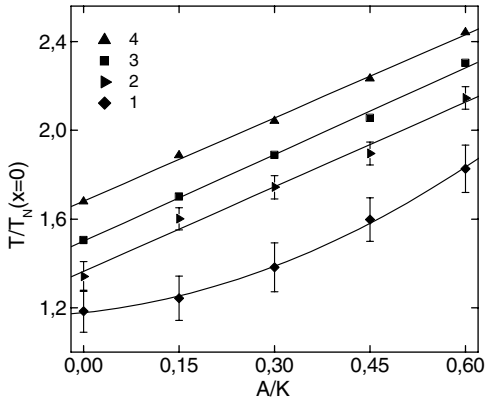

Figure 6. Curie temperature normalized to the Néel temperature of A-type AFM versus the four-spin exchange value for $x = 0.1$ (1), 0.2 (2), 0.3 (3), 0.5 (4).

dependence is fitted well by the linear expression $(T_c(A) - T_c(x, A = 0))/T_N(x = 0) = 0.6A/K$ at $x > 0.1$. Using the critical concentration of the AFM–FM transition and the $T_c(A)$ dependences, the two exchange parameters K and A can be evaluated. Satisfactory agreement with $T_{c(N)}(x)$ from experimental data [1] is observed at $x < 0.2$, $K/J = 3$ for $La_{1-x}Sr_xMnO_3$ and $x < 0.25$, $K/J = 2$ for $La_{1-x}Ca_xMnO_3$ without using four-spin exchange (see figure 7). For larger doping concentrations the best agreement with experimental data is observed when taking into account four-spin exchange. The Néel and Curie temperatures for $La_{1-x}A_xMnO_3$ (A = Ca, Sr) are satisfactorily described in terms of a model including a variation of exchange on the surface separating the La–Ca (Sr) ions with four-spin exchange $A/K = 0.15$ for Ca and $A/K = 0.2$ for Sr.

A change in the conductivity type from semiconductor to metallic is observed at $x_{c2}^{ex} = 0.225$ [7] for doping La by Ca and at $x_{c2}^{ex} = 0.175$ [1] for doping La by Sr. For $x > x_{c2}$

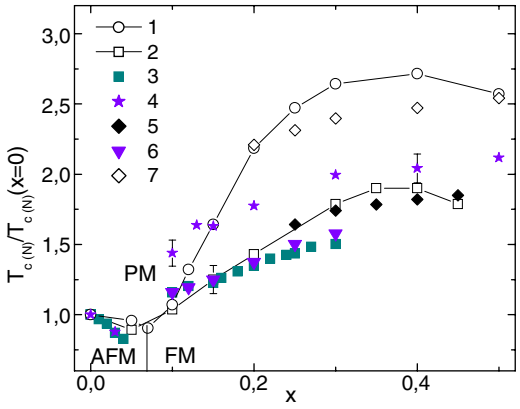

Figure 7. Phase diagram of antiferromagnetic (AFM), ferromagnetic (FM) and paramagnetic (PM) states in plane $T_{c(N)}/T_{c(N)}(x = 0)$—A = Sr, Ca ion concentration (x). Experimental data A = Sr (1), Ca (2) [1], MC results $A = 0$ $K/J = 2$, (3), $K/J = 3$ (4), $K/J = 2$, $A = 0.15$ (5), $A = 0.05$ (6), $K/J = 3$, $A = 0.3$ (7).

the main contribution to the four-spin exchange value is attributed to electron hopping. Our non-Heisenberg exchange values are essentially less as compared to the second critical value $A_{c2}/K \sim (3\text{–}4)S^{-2} \approx 1.2$, at which a quantum quadruple state is formed [8]. With increasing four-spin exchange value the type of magnetic phase transition varies from continuous to discontinuous. The critical value A_c depends on the concentration and agrees with the analytical results for the uniform system $A_{c1}/K \approx 0.5$ [9] at $x \geqslant 0.3$.

The inverse susceptibility in the Landau theory is given by

$$\chi_T^{-1} = a(T) + b(T)M^2 + c(T)M^4 + \cdots \tag{2}$$

where $a(T)$, $b(T)$, etc are coefficients determining the nature of the magnetic system. These coefficients are necessarily positive above T_c for the continuous transition. An inspection of the sign of the slope of the isotherms of H/M versus M^2 will then give the type of phase transition: positive for second order and negative for first order ($b < 0$). This criterion was applied to determine the change in the order of the phase transition in $La_{1-x}Ca_xMnO_3$ [6]. Figure 8 presents the corresponding isotherms for $x = 0.3$ and $|T/T_c - 1| = 0.1$. The isotherms intercept the M^2 axis and $(a/b) < 0$ at $T < T_c$. It is interesting to note that external field suppress the thermal magnetization fluctuations and results in a change in sign of $a(T)$ at $T > T_c$ for $M^2 > \tau^{2/3}$, $\tau = 1 - T/T_c$.

The unusual behaviour of $M(H)$ isotherms has been discussed by Aharony and Pytte [10] in a model with random field, in which the magnetization vanishes but the zero-field susceptibility is infinite, because of algebraically decaying correlations. Burgy [11] has considered the cooperative nature of the lattice distortions in manganites as a random field. Rivadulla *et al* [6] has explained the nondivergence of the susceptibility at T_f from the influence of finite size effects on the spin-correlation function. In a real system the correlation length ξ is limited by the system size L, and χ $(H = 0, T)$ will saturate when ξ becomes comparable to L [6]. Four-spin interaction will break the magnetic ordering in domains of a certain size L, when the A value is less than the FM exchange [12].

The temperature dependence of resistivity in manganites is closely related with the $M(T)$ magnetization [13]. The simulated Monte Carlo magnetization presented in figure 9 is in agreement with the prediction of the double exchange model for $t/T_c = 8$, with carrier density $n \approx 0.5$ [14]. The magnetization data can be fitted with a power law of $M(T) \sim |1 - T/T_c|^{\beta}$

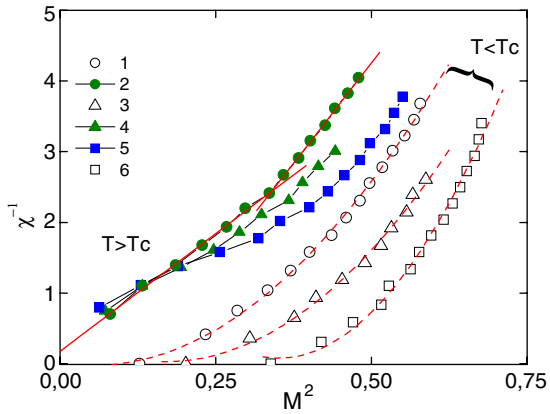

Figure 8. H/M versus M^2 plots for various four-spin exchange parameters $A/K = 0$ (1, 2), 0.15 (3, 4) 0.2 (5, 6) around T_c for $|T/T_c - 1| = 0.1$. MC results were approximated by the polynomial of equation (2) (dashed line) and with a linear expression (solid line).

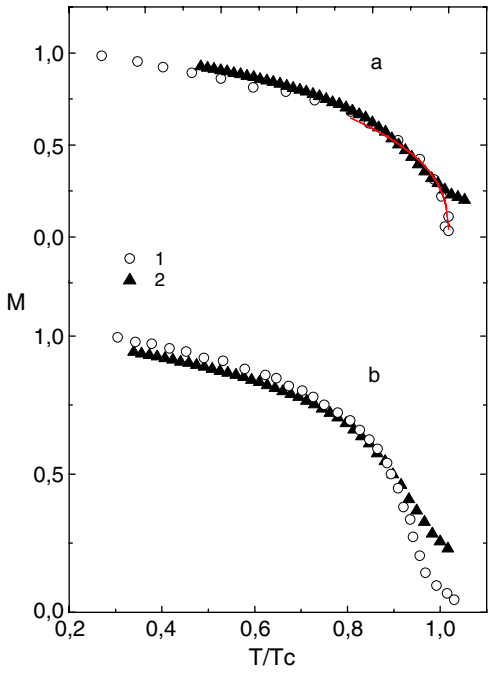

Figure 9. Temperature dependence of magnetization $M(T)$ simulated for $x = 0.3$, $K/J = 2$, $A/K = 0.15(2)$, double-exchange model [14] (1) (a), $K/J = 3$, $A/K = 0.2$ (solid circles) and experiment (1) (b) versus T/T_c.

just below T_c. The solid line in figure 9 is the fitting curve, yielding $\beta = 0.37 \pm 0.03$. More precise determination requires finite size scaling since the finite size effect appears in the calculated M above T_c. Similar results are also obtained by using different Monte Carlo methods for a larger size, $20 \times 20 \times 20$ [15]. Satisfactory agreement of $M(T)$ is also observed with $La_{0.7}Sr_{0.3}MnO_3$ single crystal [16], as shown in figure 9(b).

The dependence of the Curie temperature on x is also described within the s–d model with spin polarons [17]. In this model the electrons localize below the mobility threshold, inside a band with rectangular shape of the density of states and the bandwidth W. T_c satisfies the equation $T_c \approx 0.05Wc(1-c)$, $c(x) = (x^2+\delta x+3\delta)/(x+\delta)$ [18], where δ is the concentration

of cation vacancies. A reasonable agreement with the experimental data has been obtained for $\delta = 0.06$–0.072, $W \sim 2$ eV. But single crystals of $La_{1-x}A_xMnO_3$ (A = Ca, Sr) do not reveal such high defect concentration. The phase diagrams of manganites (Néel–Curie temperatures) have been explained by combining the orbital–polaron picture with lattice polarons at low and intermediate doping levels [19]. However, the temperature dependence of magnetization has a sharp drop up to $x = 0.35$. At large x the conventional double-exchange picture is recovered.

In most theoretical approaches the Mott–Hubbard model or an approximation of a virtual crystal have been used. For doping of manganites the disorder plays an important role. Since the thermodynamic properties of the carrier liquid are relatively weakly perturbed by scattering, its effect on the carrier-mediated ferromagnetism can be neglected to a first approximation. When the disorder increases and the metal–insulator transition (MIT) is approached, the mean free path (l_e) becomes comparable to the inverse Fermi wavevector. The free energy should be averaged over possible impurity distributions. Equivalently, the diffusive character of carrier transport leads to exponential dumping of the RKKY interaction at distances longer than l_e. However, large fluctuations in the carrier distribution have to be taken into account at criticality and on the insulator side of the MIT. The interplay between Anderson–Mott localization, Stoner magnetism, and carrier-mediated spin–spin interaction creates huge difficulties in evaluating the exchange interactions. Therefore for describing the magnetic properties of manganites we may apply a spin Hamiltonian with effective exchange parameters. The existence of four-spin interactions indicates the key importance of many-particle effects in manganites. The relevant contribution to transport properties of manganites may be due to two-electron excitations.

Summing up, the magnetic properties of manganites such as the Curie and Néel temperatures versus doping concentration are impossible to explain using only bilinear exchange parameters. The substitution of the rare-earth ion by a bivalent ion in $La_{1-x}A_xMnO_3$ (A = Ca, Sr) causes the formation of ferromagnetic exchange between manganese ions having the value $K/J \approx 2$, and four-spin exchange $A/K = 0.15$ for doping La by Ca and $K/J = 3$, $A/K = 0.2$ for doping La by Sr. Formation of the four-spin exchange arises from carrier hopping and coincides with the critical concentration metal–dielectric transition. The saturation concentration of FM bonds over the surface of separation between La^{3+} and $Ca^{2+}(Sr)^{2+}$ is in agreement with the concentration of MI transition.

References

[1] Salamon M B and Jaime M 2001 *Rev. Mod. Phys.* **73** 583
[2] Millis A J, Littlewood P B and Shraiman B I 1995 *Phys. Rev. Lett.* **74** 5144
[3] Okuda T *et al* 1998 *Phys. Rev. Lett.* **81** 3203
[4] Coey J M D, Viret M and Ranno L 1995 *Phys. Rev. Lett.* **75** 3910
[5] Lawler J F, Lunney J G and Coey J M D 1994 *Appl. Phys. Lett.* **65** 3017
[6] Rivadulla R, Rivas J and Goodenough J B 2004 *Phys. Rev.* B **70** 172410
[7] Biotteau G *et al* 2001 *Phys. Rev.* B **64** 104421
[8] Matveev V M 1973 *Zh. Eksp. Teor. Fiz.* **63** 1626
[9] Adler J and Oitma J 1979 *J. Phys. C: Solid State Phys.* **12** 575
[10] Aharony A and Pytte E 1980 *Phys. Rev. Lett.* **45** 1583
[11] Burgy J, Moreo A and Dagotto E 2004 *Phys. Rev. Lett.* **92** 097202
[12] Sandvick A W, Daul S, Singh R R P and Scalapino D J 2002 *Phys. Rev. Lett.* **89** 247201
[13] Furukawa N 1994 *J. Phys. Soc. Japan* **63** 3214
[14] Hongsuk Yi, Hur N H and Yu J 2000 *Phys. Rev.* B **61** 9501
[15] Calderon M J and Brey L 1998 *Phys. Rev.* B **58** 3286
[16] Ghosh K *et al* 1998 *Phys. Rev. Lett.* **81** 4740
[17] Laiho R *et al* 2000 *J. Phys.: Condens. Matter* **12** 5751
[18] Varma C M 1996 *Phys. Rev.* B **54** 7328
[19] Khaliullin G and Kilian R 1999 *Phys. Rev.* B **60** 13458